

High-temperature heat capacity and thermodynamic functions of zinc telluride

K.S. Gavrichev^{a,*}, G.A. Sharpataya^a, V.N. Guskov^a, J.H. Greenberg^b,
T. Feltgen^c, M. Fiederle^c, K.W. Benz^c

^aKurnakov Institute of General and Inorganic Chemistry, RAS, Leninsky pr., 31, Moscow 117907, Russia

^bDepartment of Inorganic Chemistry, Hebrew University, 91904 Jerusalem, Israel

^cKristallographisches Institut, Universitat Freiburg, Hebelstr., 25, 79104 Freiburg, Germany

Received 1 June 2001; received in revised form 21 June 2001; accepted 15 July 2001

Abstract

High-temperature heat capacities were measured using the Setaram DSC 111 in the temperature range 290–925 K. Experimental data were smoothed jointly with earlier determined low-temperature heat capacities to calculate thermodynamic properties in temperature range 15–925 K. Extrapolation of heat capacity curve to 1500 K allows to calculate Gibbs free energy at high temperatures. © 2002 Elsevier Science B.V. All rights reserved.

Keywords: High temperature; Heat capacity; Gibbs free energy

1. Introduction

An ever growing interest in cadmium and zinc telluride-based semiconductors is associated with application of these materials in X-ray, γ - and IR-radiation detectors operating at room temperature. Because of high melting point, high vapor pressure and non-stoichiometry, crystal growth of these materials is rather a complicated procedure [1]. Fundamental thermodynamic properties, in particular, heat capacity and Gibbs free energy, are the basis for the computer modeling of crystallization, post-growth cooling and annealing parameters. For ZnTe, the thermodynamic properties are inconsistent [2–4]. Moreover, heat capacity of ZnTe at high temperature has never been

experimentally measured. In the previous publication [5], we reported heat capacity measurements of ZnTe by the adiabatic calorimetry at low temperatures (15–320 K). From these results, reliable thermodynamic properties (heat capacity, entropy, enthalpy change and Gibbs free energy) at standard conditions were derived.

In the present publication, results are presented of the first experimental measurement of the ZnTe heat capacity at high temperatures, from which reliable data on heat capacity and Gibbs free energy at temperatures up to the ZnTe melting point were obtained.

2. Experimental

Crystalline ZnTe was prepared from high-purity elements supplied by NORANDA Co., Canada. Total impurity content in the initial substances was less than

* Corresponding author. Tel.: +7-95-955-4852;

fax: +7-95-954-1279.

E-mail address: gavrich@igic.ras.ru (K.S. Gavrichev).

1 ppm. Synthesis was carried out in the pumped and sealed quartz ampoules with vibrational stirring. Samples were heated in a step-wise regime up to 1400 K and held at this temperature for 10 days. After that the material was slowly cooled down to 550 K (5 days) and annealed at this temperature for 10 days. XRD analysis (G.S. Yurjev, Institute of Inorganic Chemistry, SO RAS) showed that this procedure resulted in single phase material with cubic structure. Vapor pressure measurements at $T > 800$ K confirm that the sample composition was within the homogeneity range of ZnTe. Before loading into the calorimetric container, the sample was pulverized in an agate mortar to the grain size 0.3–1 mm.

Heat capacity of ZnTe was measured at temperatures 290–925 K using the DSC 111 Setaram scanning calorimeter. The temperature measurements were reproducible within ± 0.1 K at a temperature scale uncertainty ± 0.5 K; the maximum sensitivity was $15 \mu\text{J s}^{-1}$. Powdered ZnTe was placed in a hermetic steel container with nickel laying to prevent oxidation and sublimation of the sample.

Heat capacity of ZnTe (mass of the sample 0.4392 g) was measured using the program of step-wise heating in cycles; heating at the rate of 1.5 K min^{-1} (200 s) was followed by an isothermal arrest (400 s). This resulted in a temperature increase of 5 K min^{-1} per cycle. The measurements were conducted with successive runs of 30–35 points (cycles) overlapping in temperature. Between experimental runs, the sample was cooled in the calorimeter at the rate of $10\text{--}20 \text{ K min}^{-1}$ and held at room temperature for 15–20 h. To reach the starting temperature of the next run of measurements, the sample was heated at the rate of $5\text{--}10 \text{ K min}^{-1}$.

Since the DSC measurements were expected to be affected by the thick-wall steel container, preliminary heat capacity measurements were carried out on a standard, crushed single crystals of artificial corundum ($\alpha\text{-Al}_2\text{O}_3$). Corundum heat capacity data in the studied temperature range was fitted by the equation

$$C_p(T) = a + bT - cT^{-2} + dT^2 + eT^3 + fT^4. \quad (1)$$

Mean square-root deviation of the experimental heat capacities from those calculated according to Eq. (1) was 0.3%. Deviation of the smoothed corundum $C_p(T)$ values from the tabulated data [6] changed monotonously from 8% at 300 K to -4% at 925 K.

Accordingly, the deviation of the smoothed $C_p(T)_{\text{Al}_2\text{O}_3, \text{meas}}$ values from the tabulated data was assumed to be the systematic error $\Delta(T)$

$$\Delta(T) = \frac{[C_p(T)_{\text{Al}_2\text{O}_3, \text{meas}} - C_p(T)_{\text{Al}_2\text{O}_3, \text{lit}}]}{C_p(T)_{\text{Al}_2\text{O}_3, \text{lit}}} \quad (2)$$

The corrected ZnTe heat capacity was then calculated as

$$C_p(T)_{\text{cor}} = \frac{C_p(T)_{\text{meas}}}{[1 + \Delta(T)]} \quad (3)$$

3. Results and discussion

Results of the ZnTe heat capacity measurements in four experimental runs are given in Fig. 1 (135 points). Treatment of the data obtained in the high-temperature range and comparison with the low-temperature adiabatic calorimetry results consisted of the following steps:

- smoothing of the experimental DSC data;
- correction of the high-temperature data based on the low-temperature results;
- smoothing of the combined low- and high-temperature data;
- fitting of the $C_p(T)$ data by Maier–Kelly type equation and extrapolation of ZnTe heat capacity up to 1500 K.

1. To describe the temperature dependence of the heat capacity at high temperatures, Debye, Einstein and Kieffer (DEK) model was used in which the measured C_p is represented as a sum of different contributions. The terms of the DEK equation were calculated using DEK models. Parameters of the models and coefficients of the equation

$$C_p(T) = a \sum D(\theta_D) + bE(\theta_E) + cK(\theta_L, \theta_U) + dC_p^2(T)T$$

were calculated by mean square-root procedure [7]. The last term is related to the lattice expansion work. Smoothing of the high-temperature $C_p(T)$ data by the DEK model showed that deviation of the experimental points from the calculated results in the temperature range 300–925 K was about 1.5% (Fig. 2). Comparison of the first derivative of the heat capacity over the temperature for the

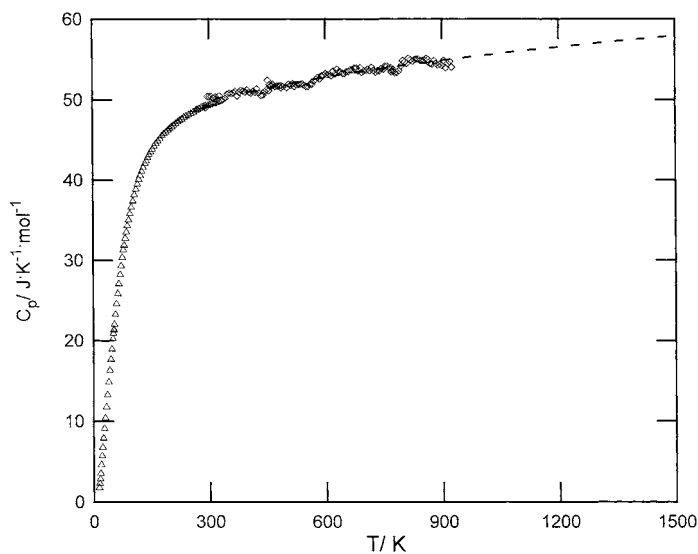


Fig. 1. Heat capacity of ZnTe in the temperature range 0–1500 K: triangles—low-temperature adiabatic calorimetry data; rhombs—DSC data; dashed line—extrapolation curve.

smoothed low- and high-temperature data in the range 290–320 K showed that the high-temperature heat capacities were systematically higher by $0.3 \text{ J K}^{-1} \text{ mol}^{-1}$ than the low-temperature data.

2. It should be stressed that systematic deviations of the DSC data from the more precise adiabatic

calorimetry measurements are observed very often and originate from the temperature gradient in the DSC cells and indeterminate heat loss. To calculate the thermodynamic properties in the wide temperature range, C_p data were reduced by $0.3 \text{ J K}^{-1} \text{ mol}^{-1}$ and listed in Table 1.

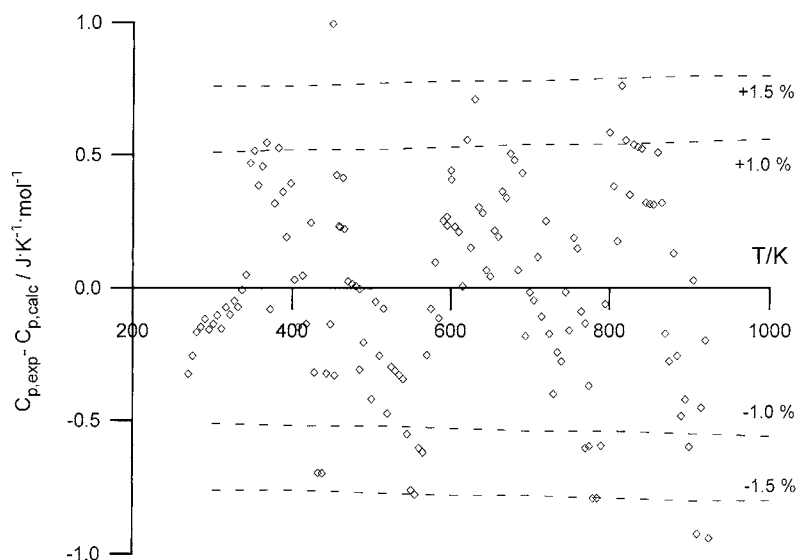


Fig. 2. Deviation of experimental heat capacity data for ZnTe in the temperature range 300–925 K.

Table 1
Experimental heat capacity of ZnTe at high temperatures (DSC measurements)

Series 1		Series 2		Series 3		Series 4	
<i>T</i> (K)	<i>C_p</i> (J K ⁻¹ mol ⁻¹)	<i>T</i> (K)	<i>C_p</i> (J K ⁻¹ mol ⁻¹)	<i>T</i> (K)	<i>C_p</i> (J K ⁻¹ mol ⁻¹)	<i>T</i> (K)	<i>C_p</i> (J K ⁻¹ mol ⁻¹)
290.7	48.73	450.2	52.45	595.0	53.09	770.0	53.51
295.9	50.14	455.2	51.93	600.0	53.31	774.8	53.55
300.9	50.05	460.2	51.79	605.0	53.14	779.8	53.39
306.0	50.15	465.2	51.84	610.0	53.16	785.0	53.42
311.1	49.96	470.2	51.69	615.0	53.00	789.8	53.65
316.1	50.12	475.2	51.73	620.0	53.59	794.7	54.21
321.2	49.73	480.2	51.77	625.0	53.22	799.9	54.89
326.3	50.23	485.2	51.81	629.9	53.82	804.9	54.71
331.4	50.00	490.2	51.66	634.9	53.46	809.6	54.54
336.5	50.13	495.2	51.51	639.9	53.48	814.7	55.15
341.6	50.25	500.2	51.54	644.9	53.30	819.9	54.98
346.7	50.74	505.2	51.96	649.9	53.31	824.7	54.80
351.7	50.84	510.2	51.81	654.8	53.52	829.7	55.02
356.8	50.78	515.2	52.03	659.8	53.54	834.9	55.04
361.9	50.87	520.2	51.68	664.7	53.74	839.8	55.06
367.0	50.06	525.2	51.90	669.7	53.76	844.8	54.89
372.1	50.50	530.2	51.94	674.8	53.96	849.9	54.91
377.2	50.95	535.2	51.97	679.8	53.98	854.7	54.94
382.2	51.22	540.2	52.00	684.8	53.60	859.7	55.16
387.3	51.12	545.1	51.84	689.8	54.00	864.8	55.00
392.4	51.01	550.1	51.68	694.7	53.42	869.8	54.54
397.4	51.27	555.1	51.70	699.7	53.62	874.8	54.46
402.6	50.96	560.1	51.92	704.8	53.63	879.8	54.89
407.6	50.84	565.1	51.95	709.8	53.83	884.7	54.53
412.7	51.09	570.1	52.36	714.8	53.64	889.7	54.33
417.8	50.97	575.1	52.58	719.8	54.03	894.8	54.42
422.9	51.41	580.1	52.80	724.7	53.64	899.7	54.27
427.9	50.90	585.1	52.63	729.8	53.45	904.7	54.93
433.0	50.58	590.1	53.03	734.9	53.64	909.8	53.93
438.1	50.63	595.1	53.06	739.8	53.64	914.8	54.50
443.2	51.06	600.1	53.28	744.8	53.63	919.7	54.78
448.2	51.30			749.8	53.82	924.7	54.06
453.3	51.16			754.8	54.20		
458.4	51.77			759.6	54.20		
463.5	52.01			764.7	53.99		
				769.8	53.98		
				774.6	53.77		

3. Smoothing of the combined low- and high-temperature data was carried out taking into account statistical weights after correction determined from errors of the adiabatic calorimetry and DSC measurements. Joint smoothing was performed using DEK method. Corresponding deviations of the experimental points obtained by adiabatic calorimetry and DSC from the calculated data were 0.3 and 1.5%, respectively. Smoothed values of the thermodynamic functions

were calculated from ZnTe heat capacity data and are listed in Table 2.

4. Extrapolation of the heat capacity curves up to 1500 K was made by two independent ways: using DEK model and Maier–Kelly type equation [8]

$$C_p = a + bX - \frac{c}{X^2} + dX^2, \quad (5)$$

where $X = T/10\,000$.

Table 2
Thermodynamic properties of ZnTe at high temperatures

T (K)	C_p° ($\text{J K}^{-1} \text{mol}^{-1}$)	S° ($\text{J K}^{-1} \text{mol}^{-1}$)	Φ° ($\text{J K}^{-1} \text{mol}^{-1}$)	$H^\circ(T) - H^\circ(0)$ (kJ mol^{-1})
300	49.54	82.25	45.35	11.07
400	50.90	96.71	56.46	16.10
500	51.96	108.2	65.70	21.24
600	52.87	117.7	73.60	26.49
700	53.64	126.0	80.50	31.81
800	54.30	133.2	86.65	37.21
900	54.87	139.6	92.18	42.67
1000	55.37	145.4	97.21	48.18
1100	55.83	150.7	101.8	53.74
1200	56.26	155.6	106.1	59.35
1300	56.69	160.1	110.1	65.00
1400	57.14	164.3	113.8	70.69
1500	57.63	168.3	117.3	76.43

Heat capacity can be adequately represented by a three-term equation with the following coefficients: $a = 48.828$, $b = 62.9227$, and $c = 0.00068451$. Extrapolation of the heat capacity up to 1500 K by the two above-mentioned procedures showed that the maximum difference in $C_p(T)$ values was $1.1 \text{ J K}^{-1} \text{ mol}^{-1}$ (Fig. 3). Such a low difference implies that the obtained data is reliable.

Coefficients of the derived Gibbs free energy (Eq. (6)) in the range 300–1500 K were calculated on the basis of the Maier–Kelly type equation for ZnTe

heat capacity.

$$\Phi(X) = a_1 + a_2 \ln(X) + a_3 X^{-2} + a_4 X^{-1} + a_5 X + a_6 X^2 + a_7 X^3, \quad (6)$$

where $X = T/10\,000$. These results are listed in Table 3 along with the data computed from Yu and Brebrick [2], Barin [3] and IVTANTERMO Database [4].

It should be noted that our experimentally measured high-temperature heat capacities are essentially lower than the estimated values [3,4]. Heat capacities of ZnTe estimated by Yu and Brebrick [2], although

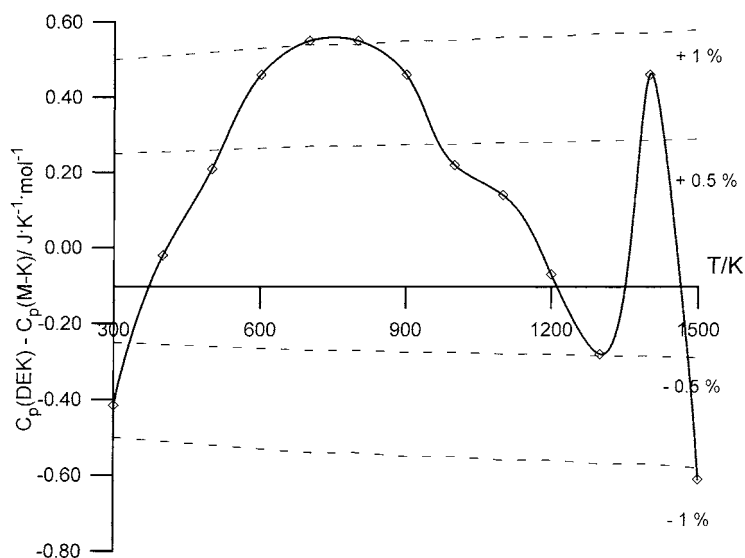


Fig. 3. Deviation of smoothed heat capacity data obtained by DEK model from Maier–Kelly type equation results.

Table 3
Comparison of Maier–Kelly equation coefficients from different sources

	Calculated from Yu and Brebrick [2]	Barin's Handbook [3]	IVTANTERMO [4]	Our data
a_1	196.966	183.088	201.7773	201.529
a_2	46.4477	44.1052	48.40199	48.828
a_3	−0.000003	0	−0.0005678	−0.0007449
a_4	0.327225	0.292964	0.4154538	0.44216
a_5	54.3321	93.6546	43.02499	38.0327
a_6	0.159626	0.37656	0	0
a_7	−0.235652	0	0	0

lower than those quoted in [3,4], are nevertheless also higher than our experimental results at $T > 600$ K.

Acknowledgements

Financial support of this work by INTAS (Grant INTAS-99-01456) is greatly appreciated.

References

- [1] F.A. Kroeger, *The Chemistry of Imperfect Crystals*, North-Holland, Amsterdam, 1969.
- [2] T.-S. Yu, R.F. Brebrick, *J. Phase Equilibria* 13 (1992) 476.
- [3] I. Barin, *Thermochemical Data of Pure Substances*, VCH, Weinheim, 1989.
- [4] L.V. Gurvich, V.S. Iorish, D.V. Chekhovskoy, V.S. Yungman, *IVTANTERMO—A Thermodynamic Database and Software System for the PC: User's Guide*, CRC press, Boca Raton, 1993.
- [5] K.S. Gavrichev, V.N. Guskov, J.H. Greenberg, T. Feltgen, M. Fiederle, K.W. Benz, *J. Chem. Thermod.*, in press.
- [6] G.T. Furukawa, T.B. Douglas, R.E. McCoskey, D.C. Ginnings, *J. Res. Natl. Bur. Stand.* 57 (1956) 67.
- [7] V.M. Gurevich, K.S. Gavrichev, V.E. Gorbunov, T.V. Danilova, L.N. Golushina, I.L. Khodakovskiy, *Geochem. Int.* 39 (2001), in press.
- [8] C.G. Maier, K.K. Kelly, *J. Amer. Chem. Soc.* 54 (1932) 3243.